

# BER Performance of Planar ESPAR Antennas in $2 \times 2$ MIMO Transmission in an Office Environment

# Hiroya TANAKA <sup>1</sup>, Jun-ichi TAKADA <sup>1</sup>,  
Atsushi HONDA <sup>2</sup>, Sorwar HOSSAIN <sup>2</sup>, Ichirou IDA <sup>2</sup>, Yasuyuki OISHI <sup>2</sup>

<sup>1</sup> Tokyo Institute of Technology

2-12-1-S6-4, O-okayama, Meguro-ku, Tokyo 152-8550, JAPAN

E-mail: {tanaka, takada}@ap.ide.titech.ac.jp

<sup>2</sup> Fujitsu Ltd.

5-5, Hikari-no-Oka, Yokosuka-shi, Kanagawa 239-0847, JAPAN

## 1. Introduction

An adaptive array antenna which can be controlled by using variable capacitors has been reported [1]. This antenna is known as the electronically steerable parasitic array radiator (ESPAR) antenna. The ESPAR antenna has an excited element and some parasitic elements, which are loaded with a variable capacitor. By controlling the bias voltages applied to the variable capacitors, the beam steering is achieved and the transmission performance can be increased. While a planar ESPAR antenna composed of patch antennas has also been reported instead of monopole antennas [2], it is better implemented on mobile applications. In this report, the bit-error-rate (BER) performance of the planar ESPAR antenna is represented in a  $2 \times 2$  MIMO transmission scheme through a measurement in an office environment.

## 2. Measurement Condition

### 2.1 Measurement Environment

The measurement was done in an indoor office environment, which is shown in Fig. 1. There were stationeries, PCs, instruments and other office supplies on the desks. Chairs, small racks and other office items were located in the aisle. The measurement was performed in a line-of-sight (LOS) and a non-LOS (NLOS) environment. The NLOS environment was emulated by putting metallic racks at the center aisle.

### 2.2 Antenna Setup

Sleeve antennas and planar ESPAR antennas were used in the Tx and Rx side, respectively. The configuration of the ESPAR antenna is illustrated in Fig. 2. The Tx antennas were placed on the desk, while the Rx antennas were on a cart. The distance between antenna elements at the Tx and Rx side were set as  $d_{Tx,ant} = 2.0\lambda$  and  $d_{Rx,ant} = 2.0\lambda$ , respectively. Further, the distance between excited and parasitic elements were set as  $d_e = 0.35\lambda$  at the ESPAR antenna. This value was determined to be well-suited from the aspect of impedance matching and beam steerable range.

### 2.3 Antenna Characteristics

In the measurement, three radiation patterns were used, which were given by the ESPAR antenna as  $(V_{VRC1}, V_{VRC2}) = (0V, 0V)$ ,  $(25V, 0V)$ , and  $(0V, 25V)$ . Therefore, the BER was measured for all combination of radiation patterns realized by two ESPAR antennas, which is nine in total.

Figure 3 shows examples of the amplitude of E-field gain where the bias voltages are  $(V_{VRC1}, V_{VRC2}) = (0V, 0V)$  and  $(0V, 25V)$ . In addition, Table 1 indicates the gain, radiation efficiency and peak radiated direction. As the radiation pattern is changed by controlling the bias voltages, the efficiency also changes because of mismatch and loss.

Table 1: Antenna gain of peak radiated direction, radiation efficiency, and peak radiated direction.

$(V_{VRC1}, V_{VRC2})$	(0V, 0V)	(25V, 0V)	(0V, 25V)
Gain [dBi]	6.7	6.8	7.0
Efficiency [%]	64	66	69
Peak direction $\phi$ [°]	6	-3	20
Peak direction $\psi$ [°]	6	6	14

Table 2: System configuration.

Center frequency	5.06 GHz
Transmitting antennas	Vertically polarized sleeve antenna $\times$ 2
Receiving antennas	Planar ESPAR antenna $\times$ 2
Modulation	OFDM-QPSK
Coding	Convolutional code
Signal detection	Zero forcing

### 3. Measurement Results

Measurement was performed under the system configuration given by Table 2. The BER was measured at 16 positions as shown in Fig. 4 at both the LOS and NLOS environments. Then, the mean BER was calculated after the measurement was finished. Moreover, while keeping the transmit power constant, noise was added to the IF signals by using the coupler and noise source, as illustrated in Fig. 5, so as to change the signal-to-noise-ratio (SNR).

Following the measurement above, the BER performances of each environment are plotted in Figs. 6 and 7. We can see that the BER drastically changes depending on the bias voltages. Although the ESPAR antenna loss was brought by the variable capacitors, the BER improves through beam selection. Therefore, it is obvious that the adaptive beam steering is effective from the viewpoint of BER performance in this environment.

### 4. Conclusion

This report represents the BER characteristics provided by the planar ESPAR antennas in  $2 \times 2$  MIMO transmission through a measurement in an office environment. In various realistic situations of using mobile systems, the antenna orientation, position, and direction of arrival change easily. This kind of change has a great influence on the transmission quality. In this report, however, it is revealed that the adaptive beam control has a possibility to improve the BER performance. In future works, the measurement has to be carried out in other environments for further assessment of the adaptive beam selection.

### Acknowledgments

This research is supported by the National Institute of Information and Communications Technology of Japan.

### References

- [1] T. Ohira and K. Gyoda, "Electronically steerable passive array radiator antennas for low-cost analog adaptive beamforming," IEEE Int. Conf. Phased Array Syst. Thec., pp.101–104, Dana Point, May 2000.

[2] H. Tanaka, J. Takada, A. Honda, I. Ida, Y. Oishi, "Capacity Analysis by Planar ESPAR Antenna in MIMO Transmission," IEEE Region 10 Conference (TENCON2006), Hong-Kong, SS1.4, Nov. 2006.

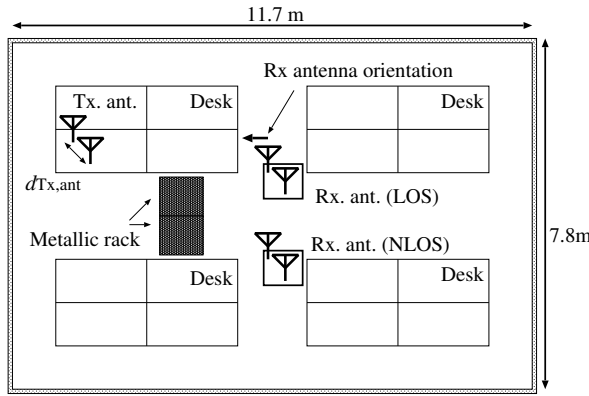


Figure 1: Measurement environment.

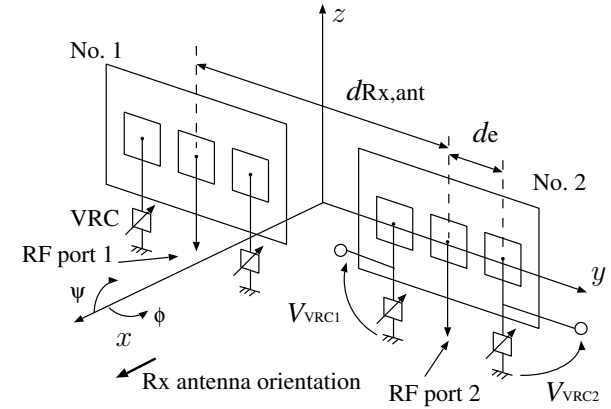
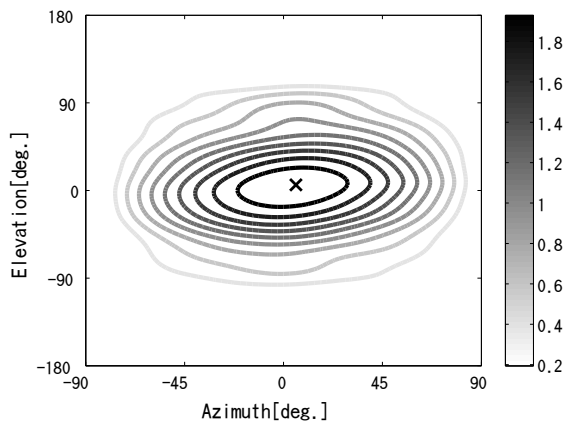
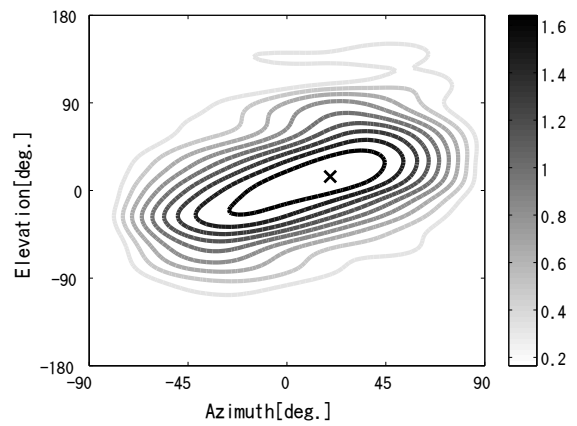


Figure 2: Antenna orientation.



(a) E-field of vertical polarization in  $(V_{VRC1}, V_{VRC2}) = (0V, 0V)$ . (x implies the peak.)



(b) E-field of vertical polarization in  $(V_{VRC1}, V_{VRC2}) = (0V, 25V)$ . (x implies the peak.)

Figure 3: Radiation patterns of the ESPAR antenna.

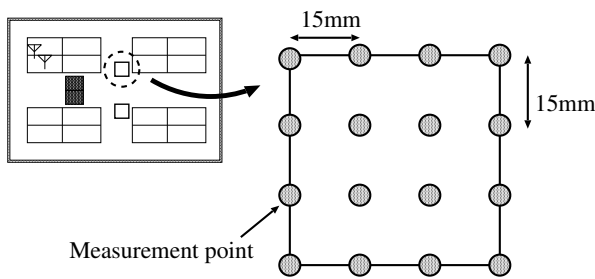


Figure 4: Measurement point in an environment.

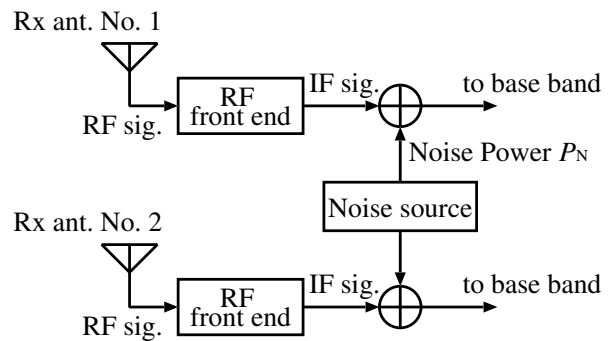


Figure 5: Noise.

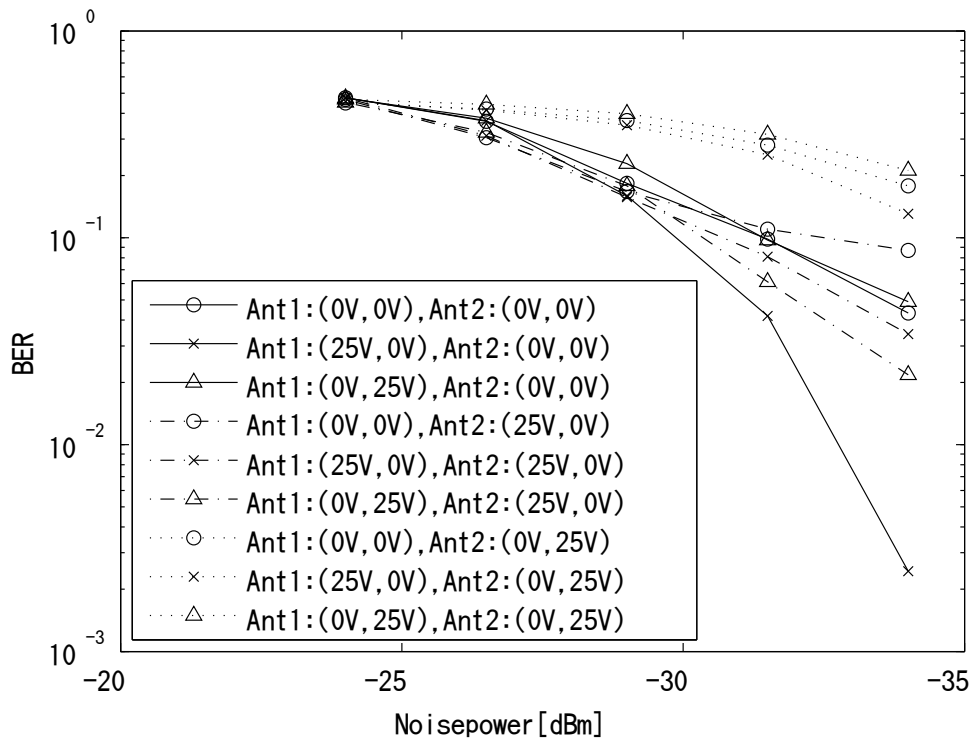


Figure 6: Mean BER measured in LOS environment.

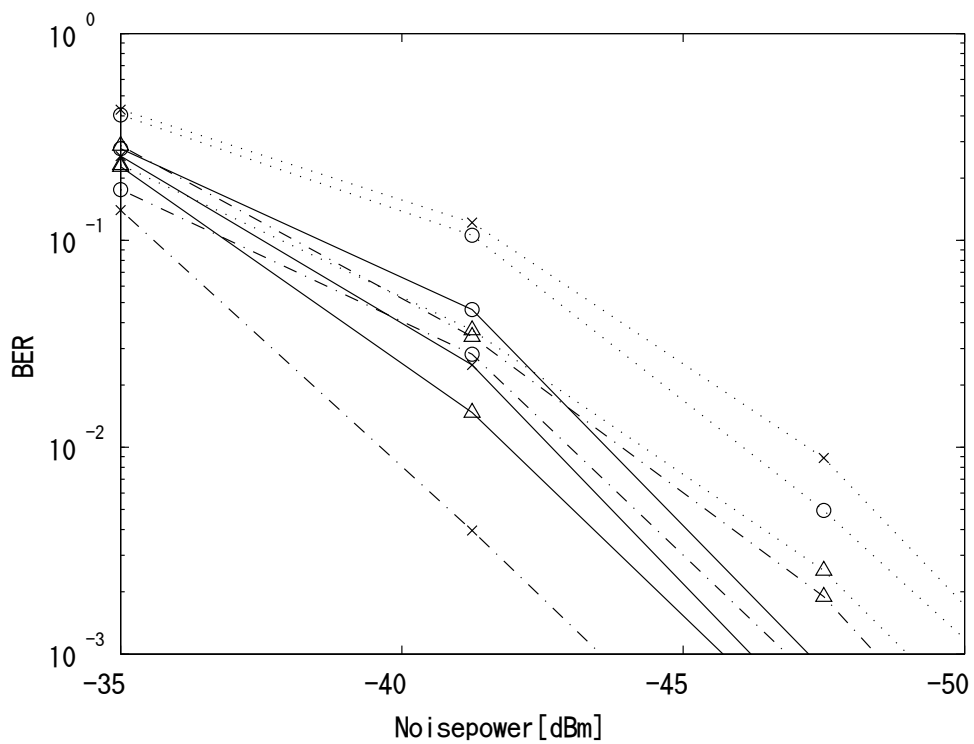


Figure 7: Mean BER measured in NLOS environment. (The legend is same as Fig. 6.)